XPCS results with the Eiger X-1M



Mark Sutton
McGill University

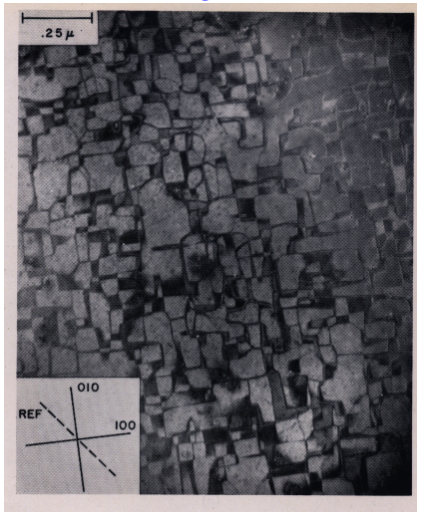
Collaborators

- J. LhermitteMcGill University.
- A. Sandy, S. Narayanan, T. Madden,X-ray Science, APS
- R. Leheny, Johns Hopkins
- F. Khan, N. Schwarz,Engineering Support, APS

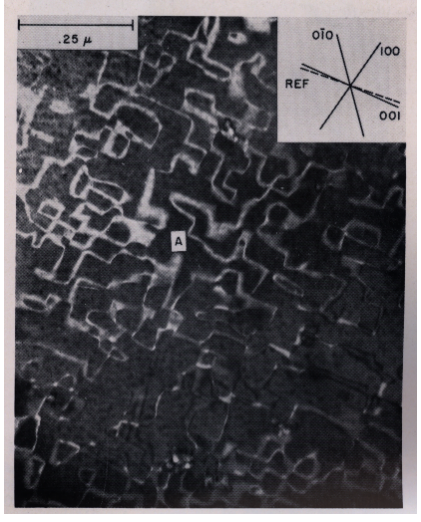
Outline

1. Introduction
2. XPCS
3. Setup
4. Measurements
5. Visibility
6. Conclusion

Cu_3Au



Antiphase domain boundaries in partially ordered $AuCu_3$.



Microstructure of Materials

- Microstructure affects most (*if not all*) macroscopic properties of materials.
- Length scales typical span from nanometers to microns.
- Microstructure depends on processing. i.e. it is history dependent and so is a non-equilibrium effect.

Correlations and response

$$\begin{aligned}\delta\langle\Psi_i(\vec{r},t)\rangle &= \langle\Psi_i(\vec{r},t)\rangle_h - \langle\Psi_i(\vec{r},t)\rangle \\ &= -\int_{-\infty}^{t} dt' \frac{1}{i\hbar}\int d\vec{r}' \chi_{\Psi_i\Psi_j}(\vec{r},\vec{r}',t-t')h_j(\vec{r}',t')\end{aligned}$$

Giving the response function:

$$\chi_{\Psi_i\Psi_j}(\vec{r},\vec{r}',t-t') = \Theta(t-t')\frac{i}{\hbar}\langle[\Psi_i(\vec{r},t),\Psi_j(\vec{r}',t')]\rangle$$

This has an imaginary part:

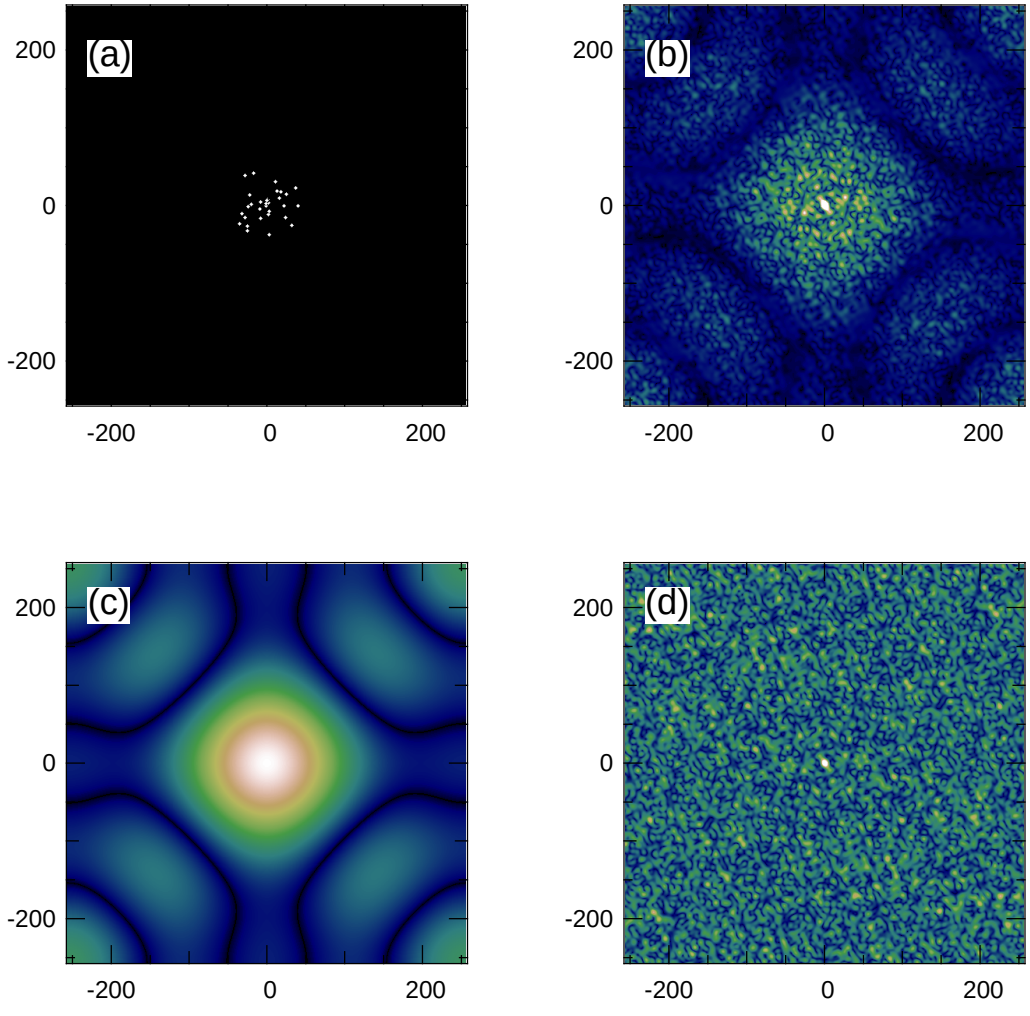
$$\begin{aligned}\chi''_{\Psi_i\Psi_j}(\vec{r},\vec{r}',t-t') &= \frac{1}{2\hbar}\langle[\Psi_i(\vec{r},t),\Psi_j(\vec{r}',t')]\rangle \\ \chi''_{\Psi_i\Psi_j}(\vec{r},\vec{r}',\omega) &= \frac{1}{2\hbar}\left(S_{\Psi_j\Psi_i}(\vec{r},\vec{r}',\omega) - S_{\Psi_j\Psi_i}(\vec{r}',\vec{r},-\omega)\right)\end{aligned}$$

where $S_{\Psi_j\Psi_i} = \langle\Psi_i(\vec{r},\omega)\Psi_j(\vec{r}',\omega')\rangle$ $(i.e. S(Q,t)$ or $S(Q,\omega))$

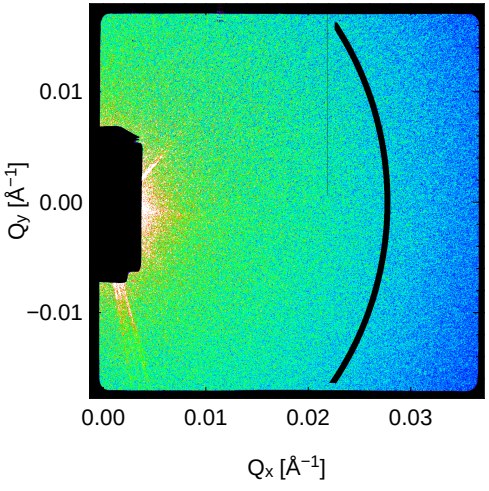
Outline

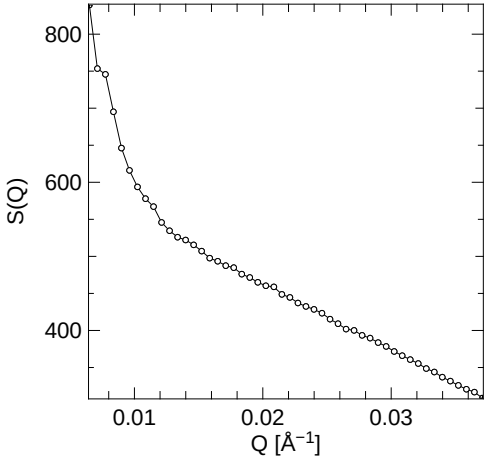
1. Introduction
2. XPCS
3. Setup
4. Measurements
5. Visibility
6. Conclusion

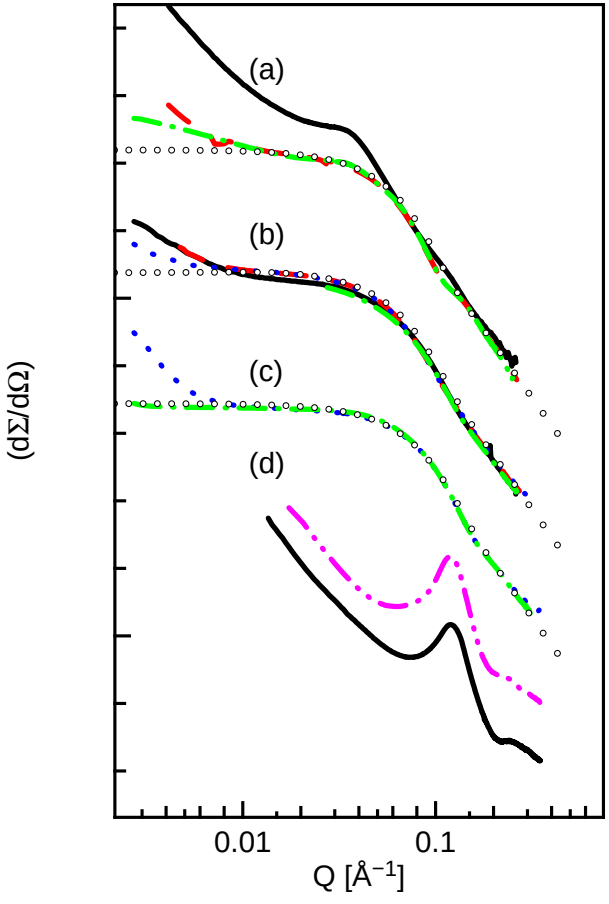
Pinholes in Tinfoil



SAXS of Au particles in PS

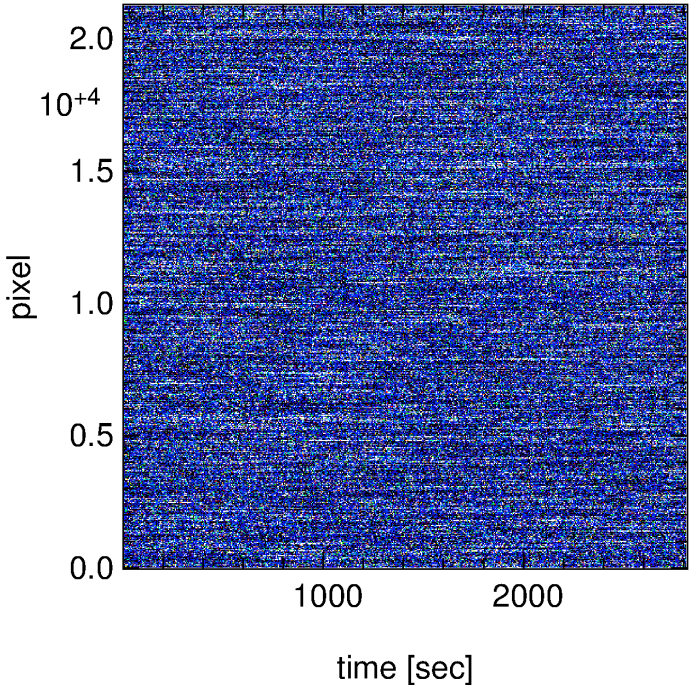






Small angle scattering of 6.0nm gold particles in polystyrene.

SAXS of Au particles in PS



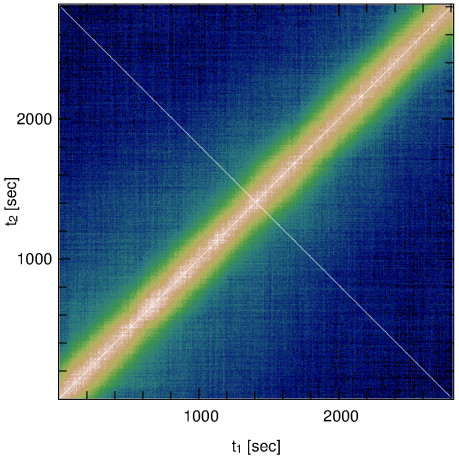
Time fluctuations in coherent scattering.

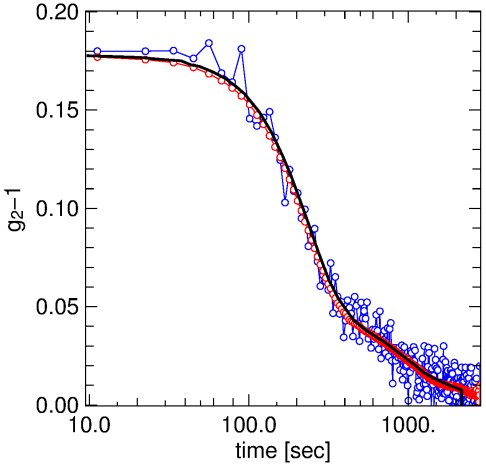
Define correlation function:

$$
\begin{aligned}
g^{(2)}(\vec{Q},\tau) \; - \; & 1 \\
= \; & \frac{\langle I(\vec{Q},t+\tau)I(\vec{Q},t)\rangle - \langle I(\vec{Q},t)\rangle^2}{\langle I(\vec{Q},t)\rangle^2} \\
= \; & \beta \left| g^{(1)}(\vec{Q},\tau) \right|^2 \\
= \; & \beta \, e^{-2\tau/\tau_Q}
\end{aligned}
$$

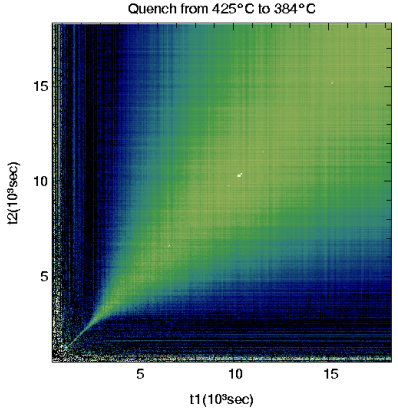
Two-time correlation functions

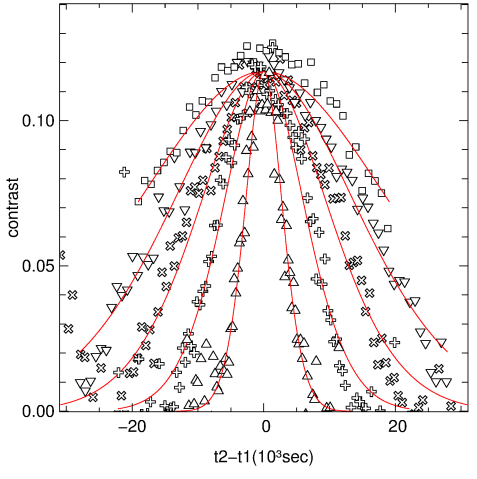
Au in polystyrene





Cu_3Au

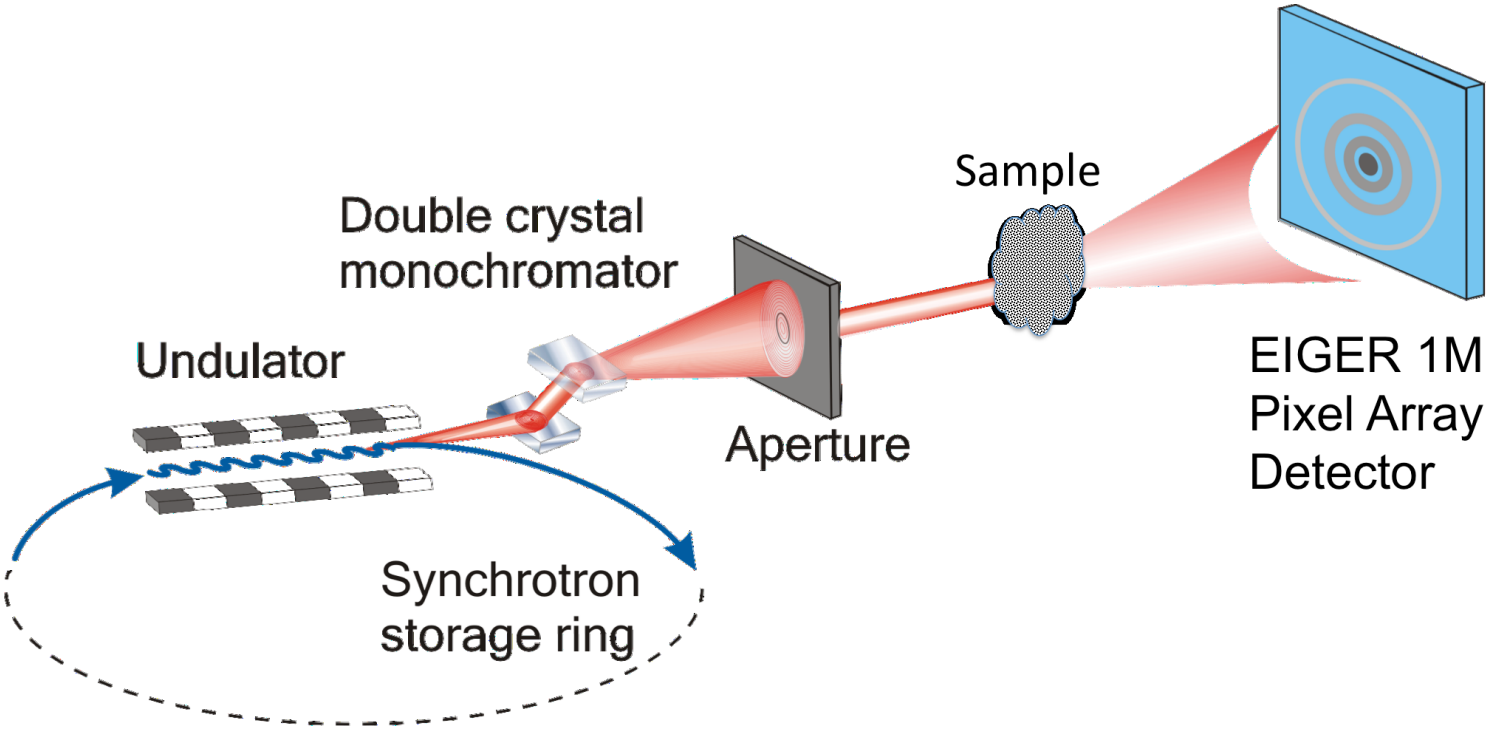




Outline

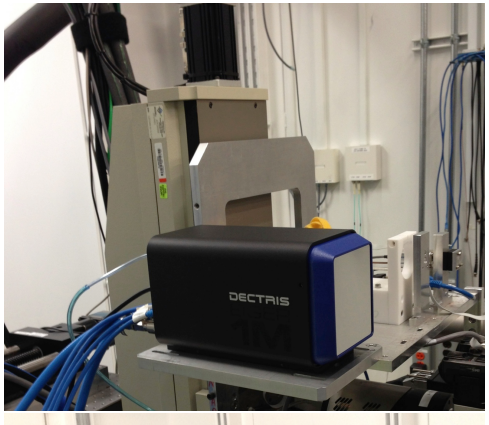
1. Introduction
2. XPCS
3. Setup
4. Measurements
5. Visibility
6. Conclusion

Coherent small angle scattering



Beamline 8IDI at Advanced Photon Source

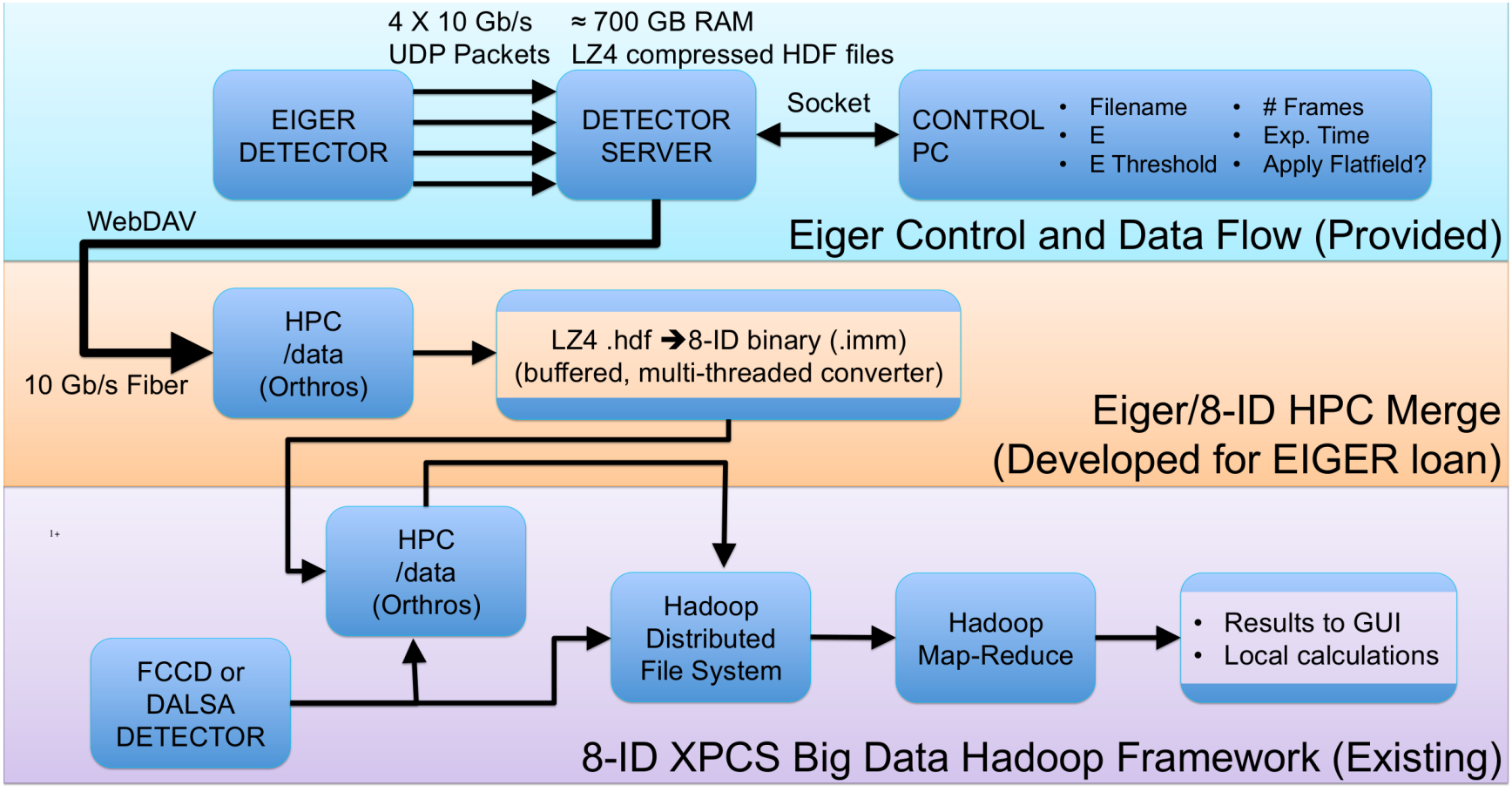
Eiger X-1M



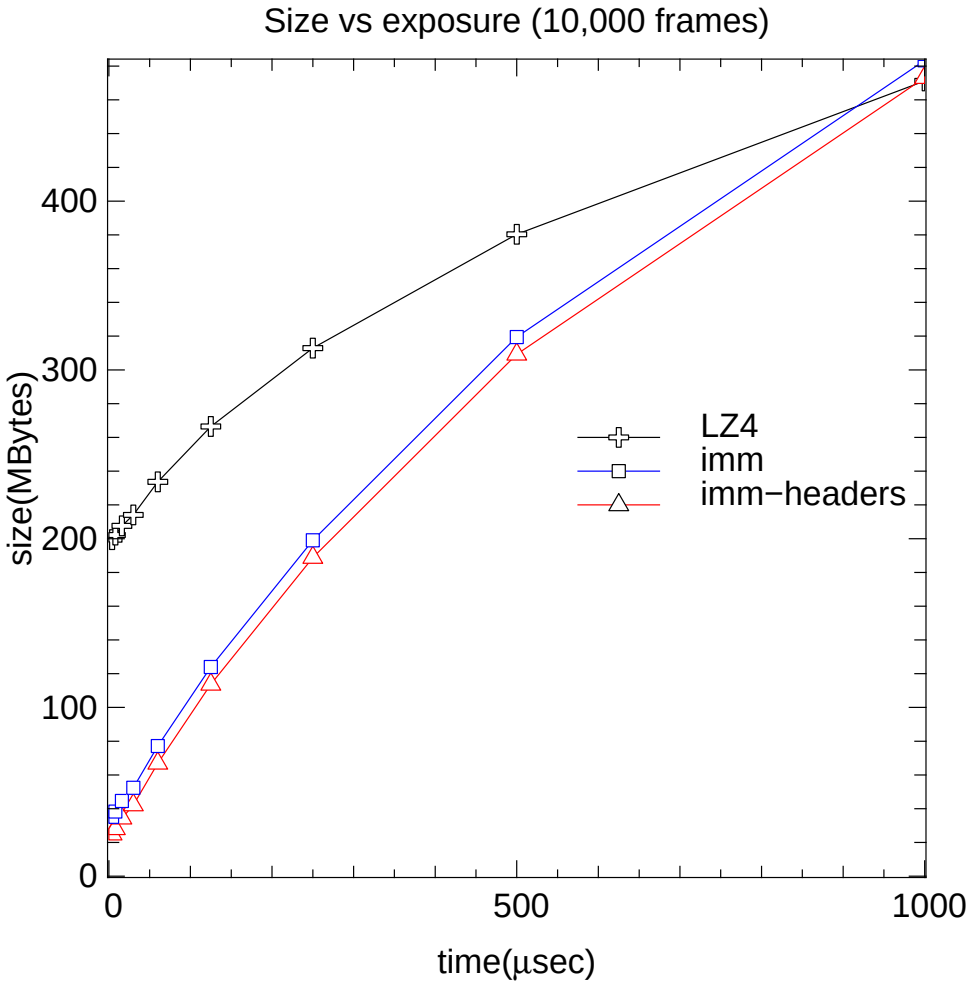


Feature	Specification
Area	1,030 x 1,065 (77 mm x 80 mm)
Sensor Thickness	300 µm (silicon)
Pixel Size	75 µm x 75 µm
Readout Speed	800 fps (prototype used) 3,000 fps (production) 3 µs deadtime
QE	1 up to ≈ 12 keV
Detector Type	Counting
Modules	1 × 2 (8 chips per module) 37 pixel gap
Counter depth	12 bits at 3 kHz
Dead area	3.5%
Weight	4 kg

Detector Setup



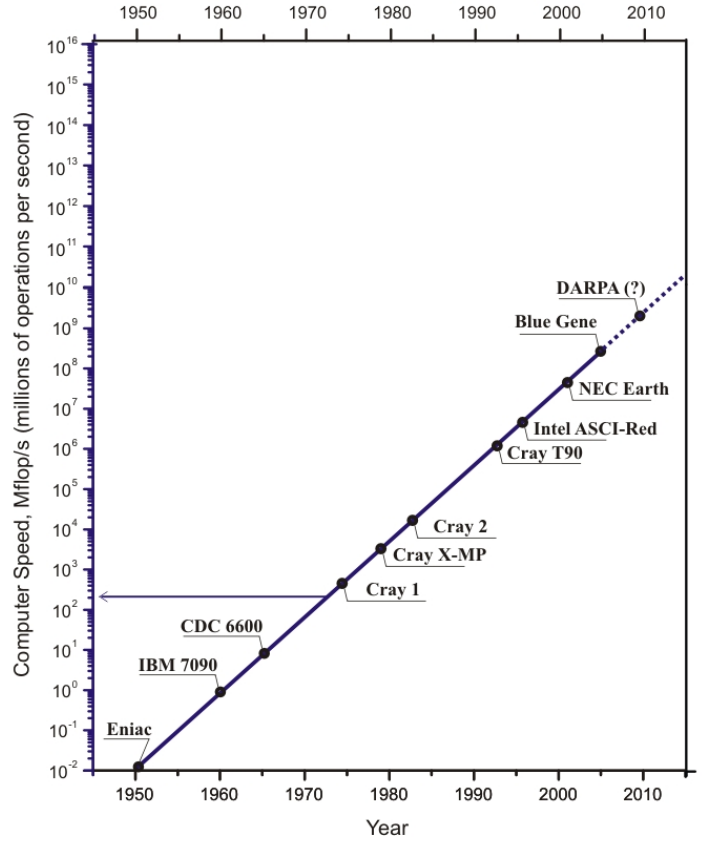
File compression



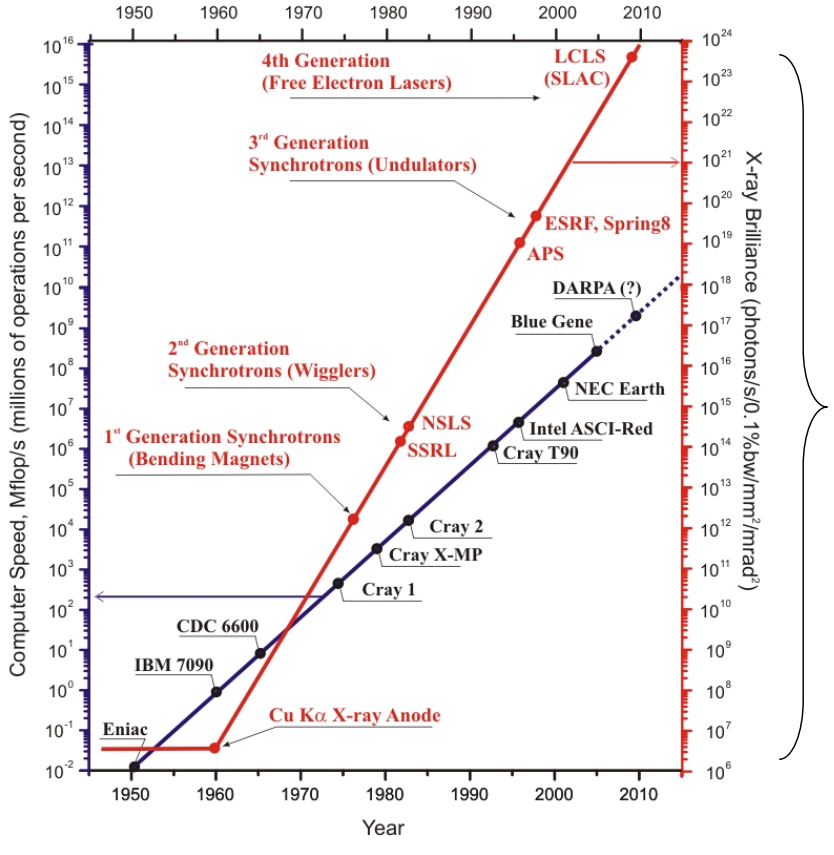
1030×1065*2*10000 is 21939 Mbytes

Moore's law for CPU chips

12 orders
of magnitude
In 6 decades



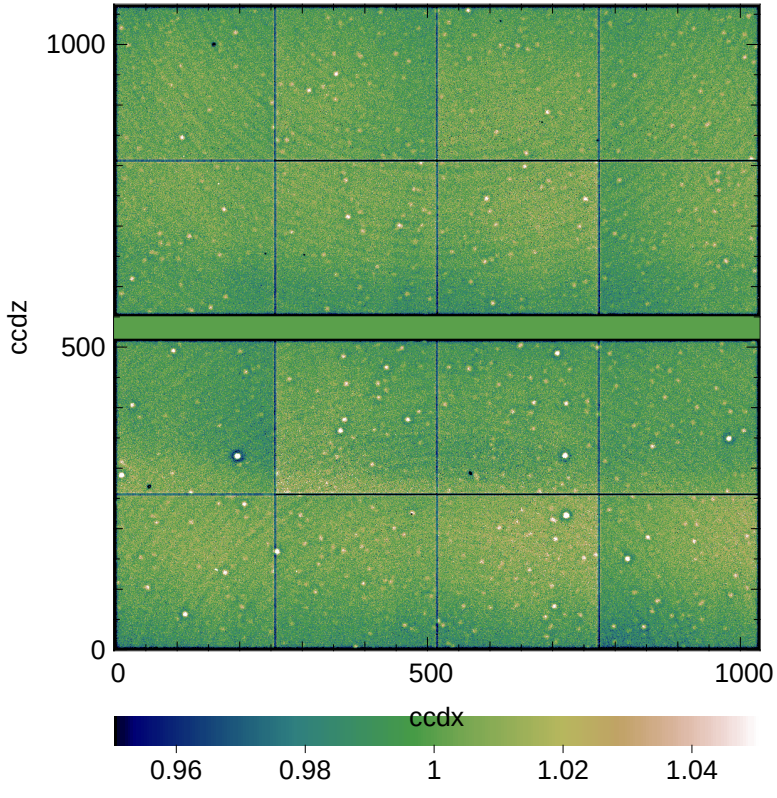
Brilliance is Coherence

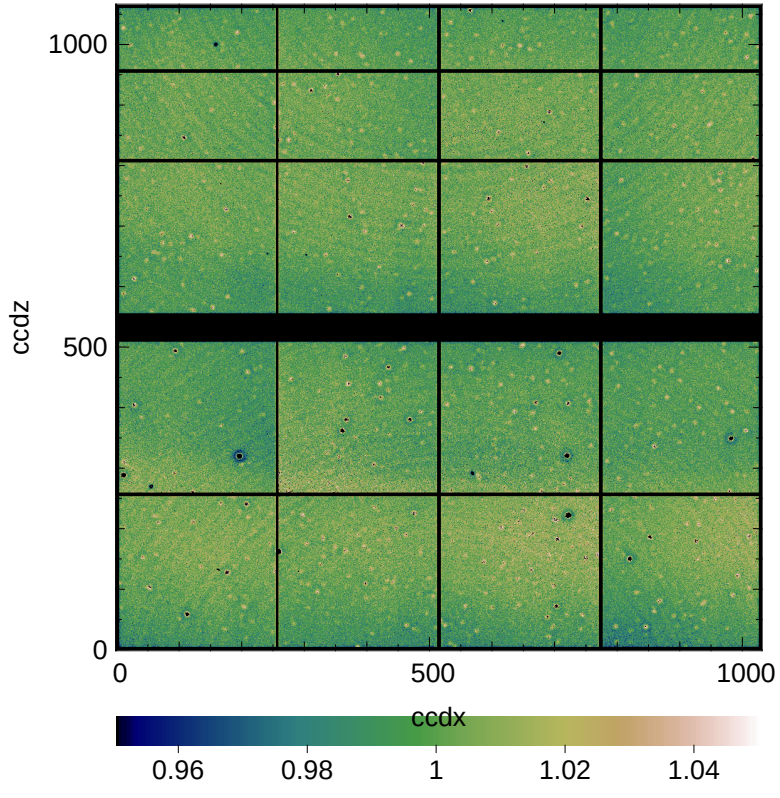


12 orders
of magnitude
In 6 decades

18 orders
of magnitude
In 5 decades!

Flatfield correction



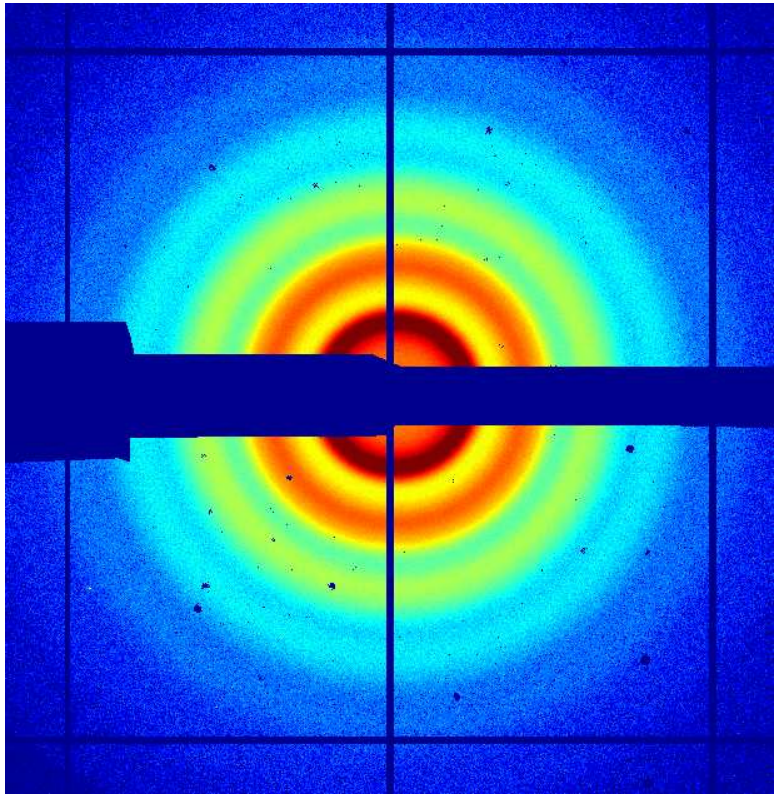


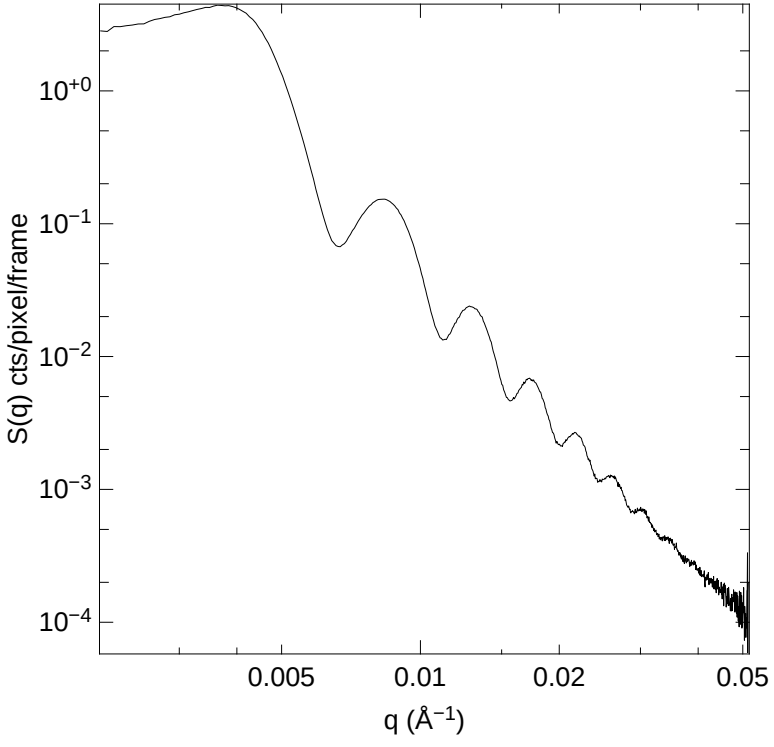
Careful with flat field correction for photon counting.

Outline

1. Introduction
2. XPCS
3. Setup
4. Measurements
5. Visibility
6. Conclusion

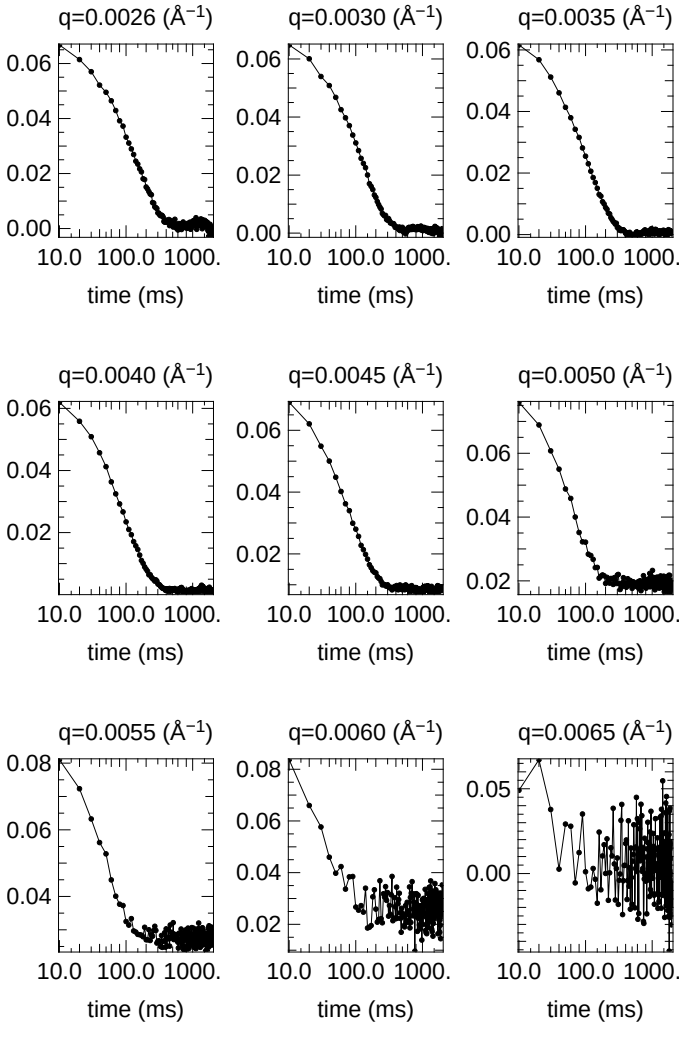
Latex spheres (70 nm, T=25 C)



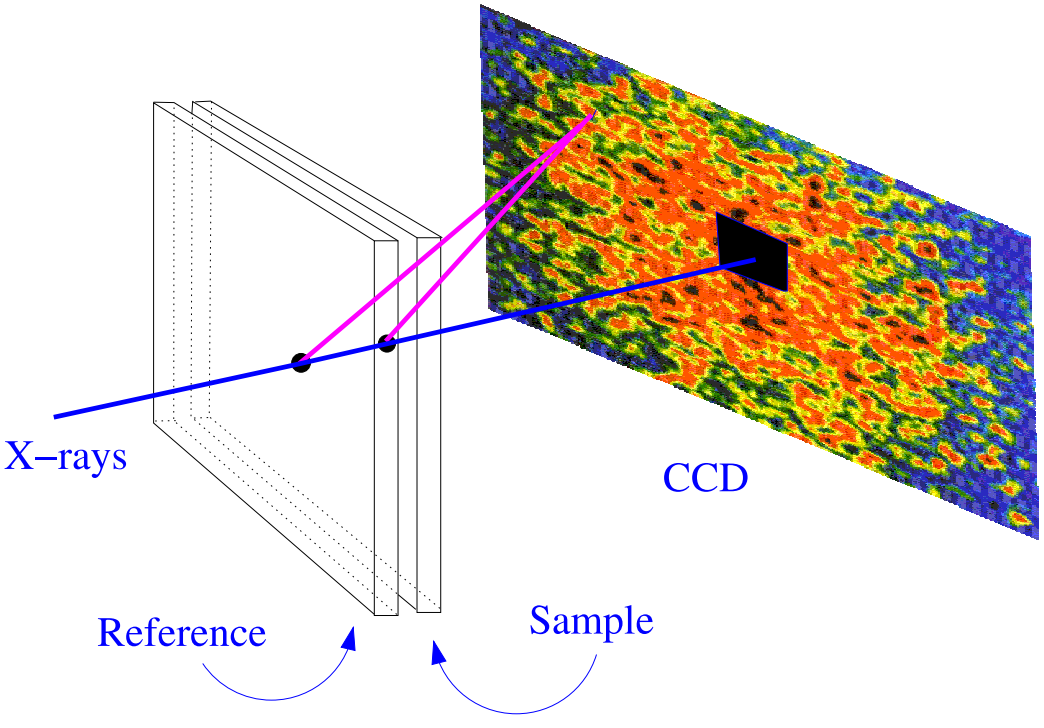


1000 frames at 10 ms (10 seconds of data)

Latex spheres (70 nm, T=25 C)



Experimental Setup



Scattering geometry

Heterodyne

$$
\begin{aligned}
G_2(\vec{q},\tau) &= \langle\ [I_r(t)+I_s(t)]\ [I_r(t+\tau)+I_s(t+\tau))]\ \rangle \\
&= I_r^2+\langle I_s(t)\rangle_t^2(1+\beta|g_1(t)|^2)+2I_r\langle I_s(t)\rangle_t+2I_r\langle I_s(t)\rangle_t\beta Re(g_1(t))
\end{aligned}
$$

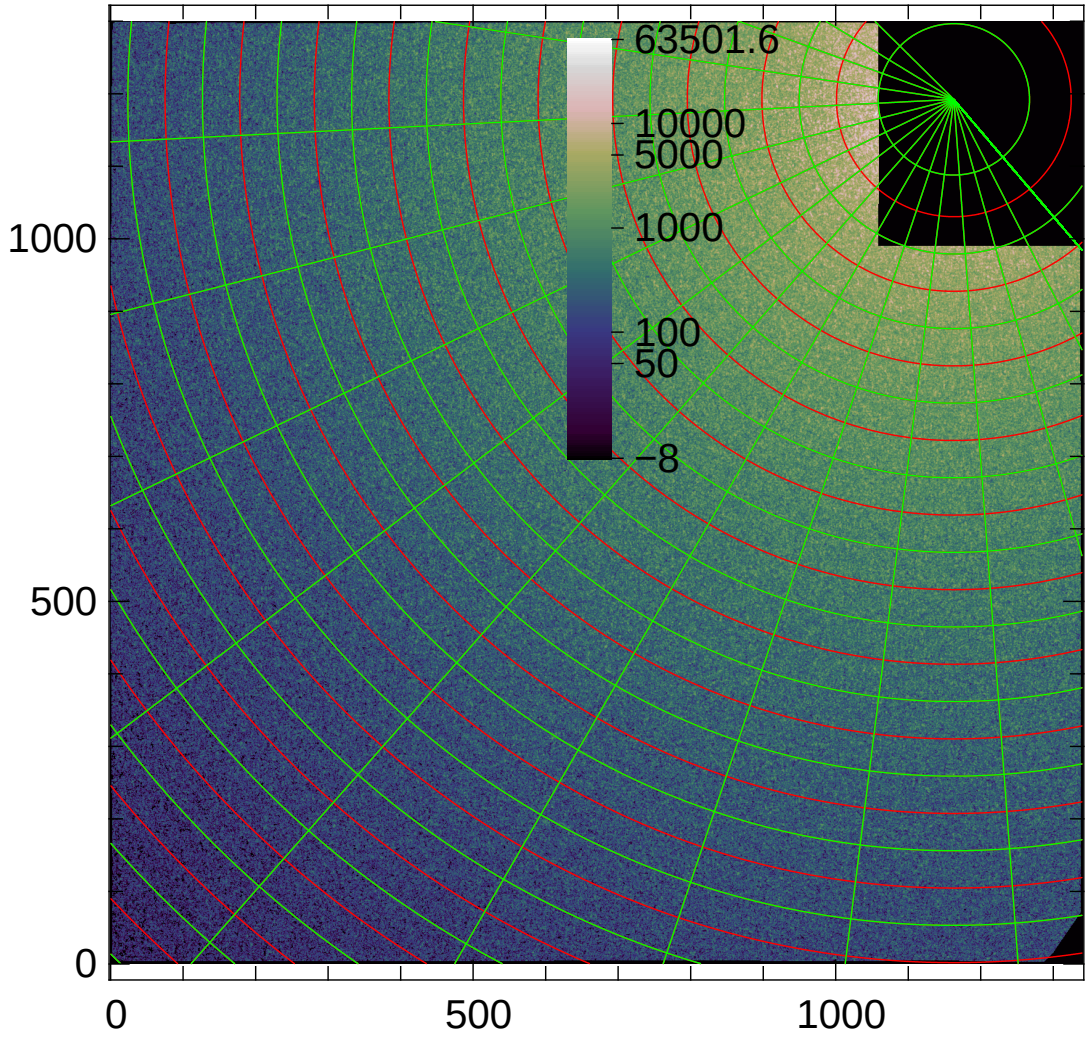
Moving at constant velocity gives phase factor

$$e^{i\vec{q}\cdot\vec{r}(t)} = e^{i\vec{q}\cdot\vec{v}t} = e^{i\omega t}$$

So correlation becomes ($x = I_s/(I_s+I_r)$)

$$g_2(q,\phi,\tau) = 1+\beta(1-x)^2+x^2\beta g_2^2(t/\tau)+2x(1-x)\beta\cos(\omega t)g_1(t/\tau)$$

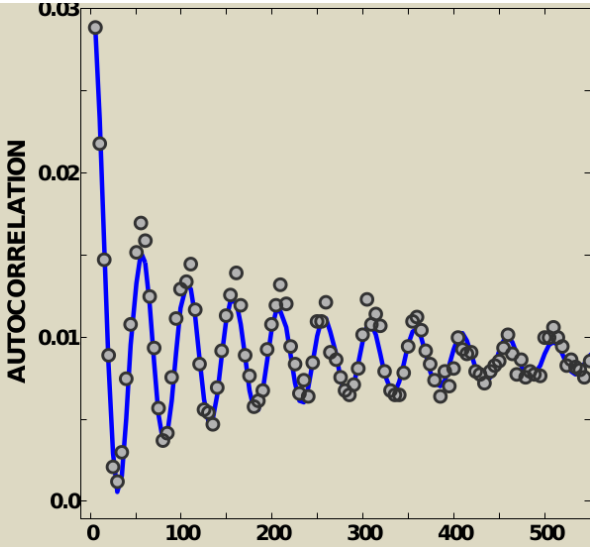
Partitioning the Scattering

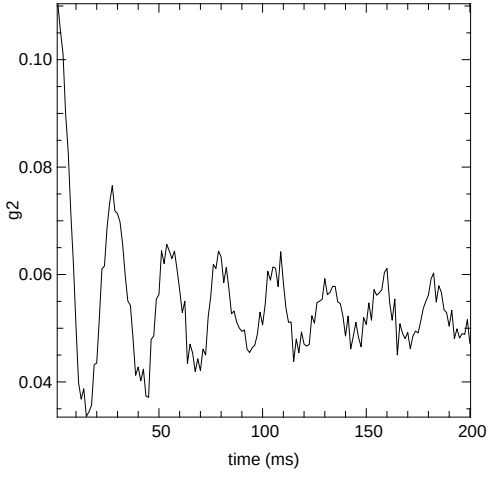


Flow measurements

Heterodyne Correlation Function

Heterodyne correlation function measured from a dense colloidal suspension flowing at 5 μm/s. Figure produced from 100,000 frames acquired at 800 fps (125 s total acquisition time).





Outline

1. Introduction
2. XPCS
3. Setup
4. Measurements
5. Visibility
6. Conclusion

Visibility

Faster than detector readout time.

$$
\begin{aligned}
g^{(2)}(\vec{Q},\tau) - 1 &= \frac{\langle I(\vec{Q},t) I(\vec{Q},t+\tau)\rangle}{\langle I(\vec{Q},t)\rangle^2} - 1 \\
&= \beta \left| g^{(1)}(\vec{Q},\tau) \right|^2 \\
&= \beta\, e^{-2\tau/\tau_Q}
\end{aligned}
$$

$$
\begin{aligned}
V_{(2)}(\vec{Q},t_c) - 1 &= \frac{\langle I^2 \rangle}{\langle I^2) - 1} \\
&= \frac{1}{\bar{I}^2 t_c^2} \left\langle \int_0^{t_c} \int_0^{t_c} I(t') I(t'') dt' dt'' \right\rangle - 1 \\
&= \frac{\beta \tau_Q^2}{2 t_c^2} \left[2\frac{t_c}{\tau_Q} - 1 + e^{-2t_c/\tau_Q} \right]
\end{aligned}
$$

Visibility

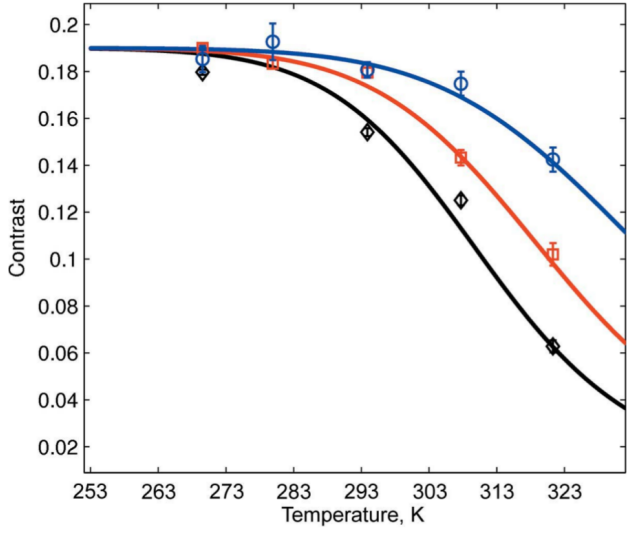


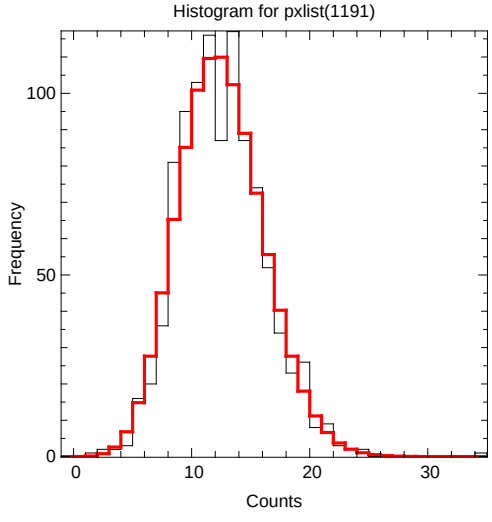
Figure 5
Speckle visibility contrast as a function of temperature for 72 nm-radius latex in glycerol; the data shown were collected at a wavevector transfer of $Q = 0.1 \pm 0.01\ \mathrm{nm}^{-1}$. Blue circles: 2 ms exposure; red squares: 5 ms exposure; black diamonds: 10 ms exposure. The 2 ms data are multiplied by a factor of 1.039 to account for the reduced contrast resulting from the shutter transit time. Solid lines are theoretical predictions based on Brownian motion.

Ref: DeCaro et al, J. Synchrotron Rad. **20**, 332-338 (2013).

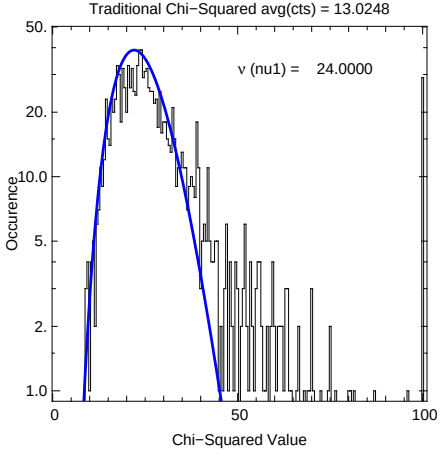
New Eiger, a counting detector has "2μs electronic shutter".

Prototype VIPIC has 153 ns framing times.

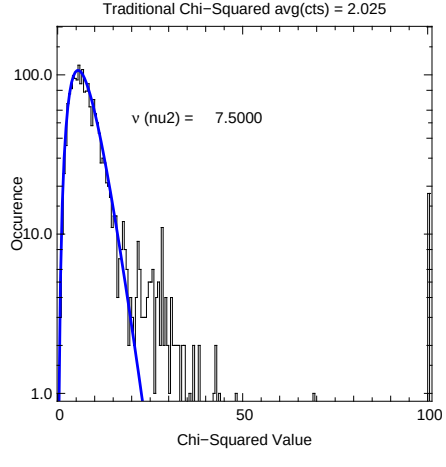
Counting Statistics



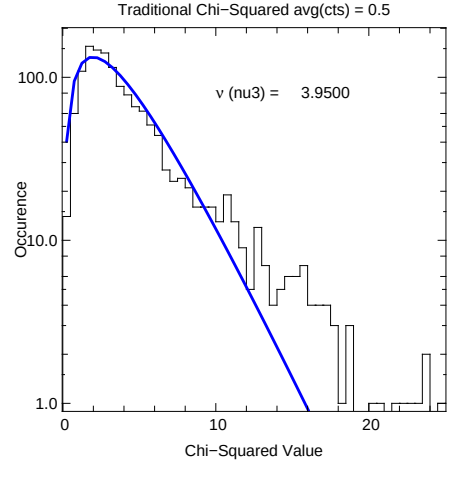
Poisson statistics



$\bar{\mu}$ = 13 cts



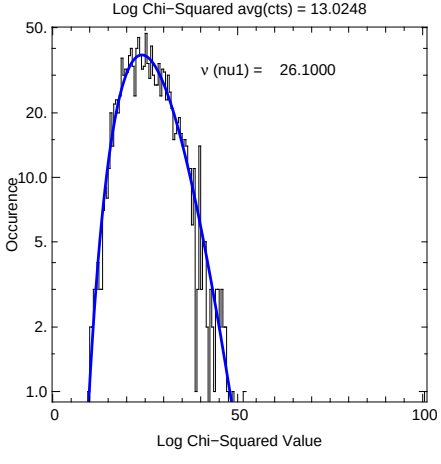
2 cts



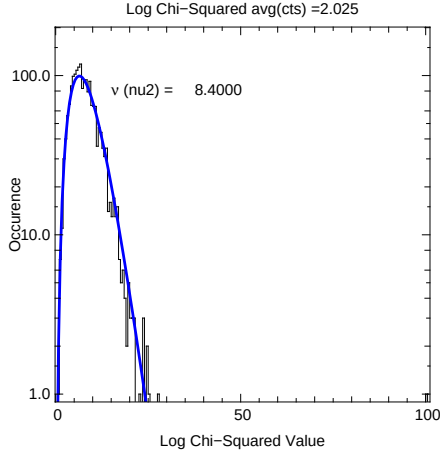
0.5 cts

Maximum Likelihood

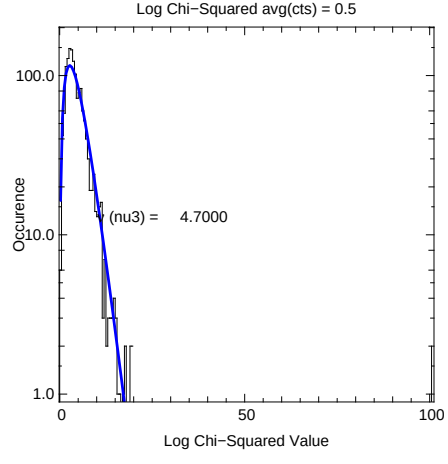
$$\chi^2 = \sum_i \frac{(n_i - Np_i)^2}{Np_i} \qquad \chi^2_L = -2\sum_i n_i \log\left(\frac{Np_i}{n_i}\right),$$



$\bar{\mu}$ = 13 cts



2 cts

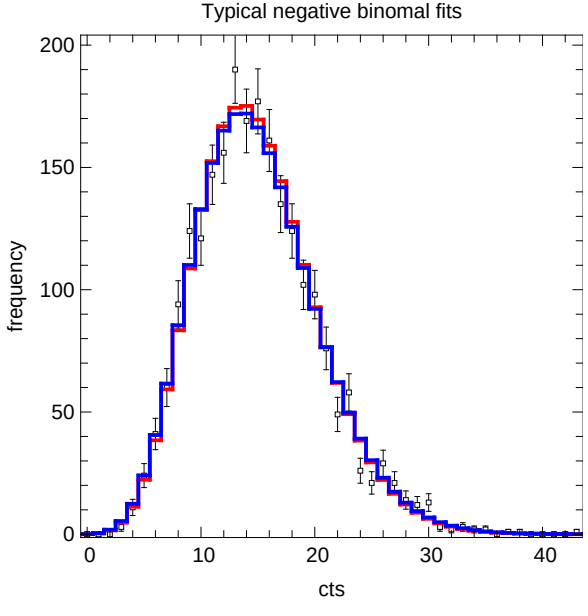


0.5 cts

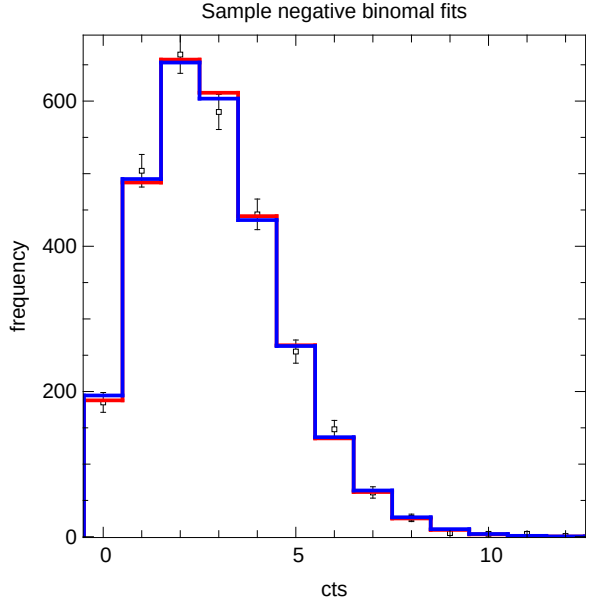
Visibility measurements

For speckle statistics are negative binomial:

$$P_i = \frac{\Gamma(i+M)}{\Gamma(M)\Gamma(i+1)}\left(1+\frac{M}{\lambda}\right)^{-i}\left(1+\frac{\lambda}{M}\right)^{-M},$$

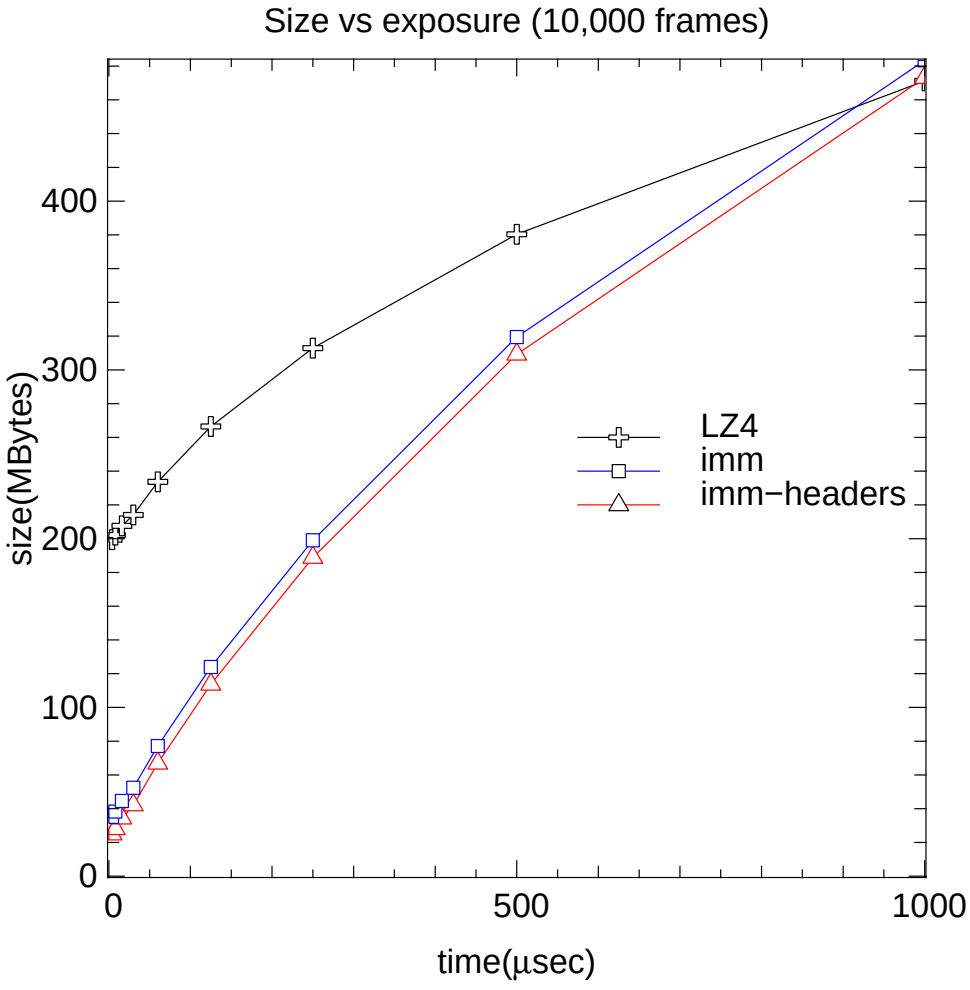


M=15.9 ± 1 (β = .062)



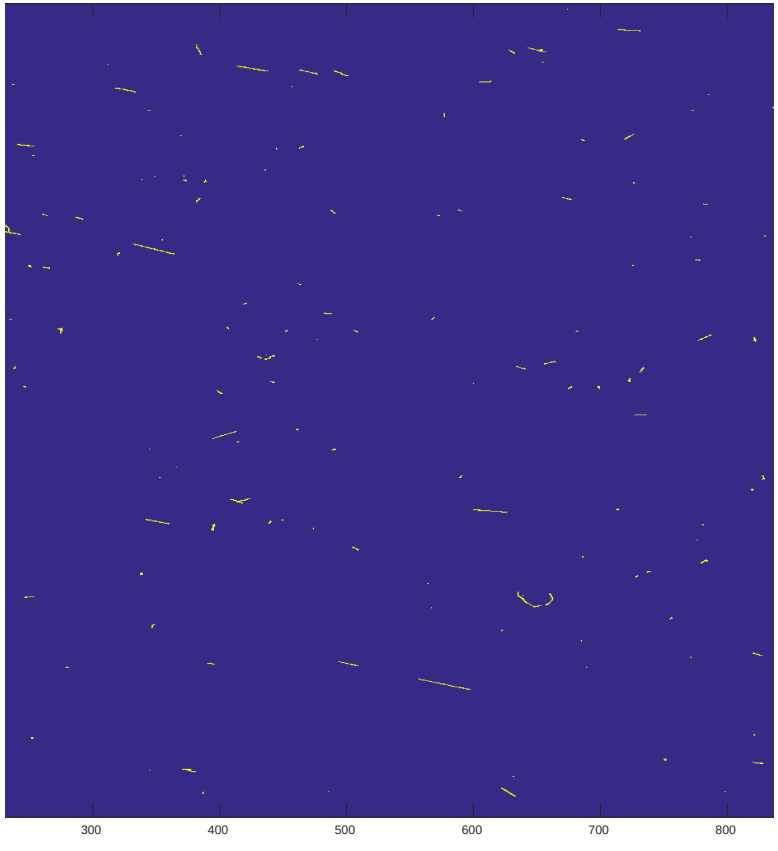
M=21.1 ± 4.5 (β = .047)

File compression



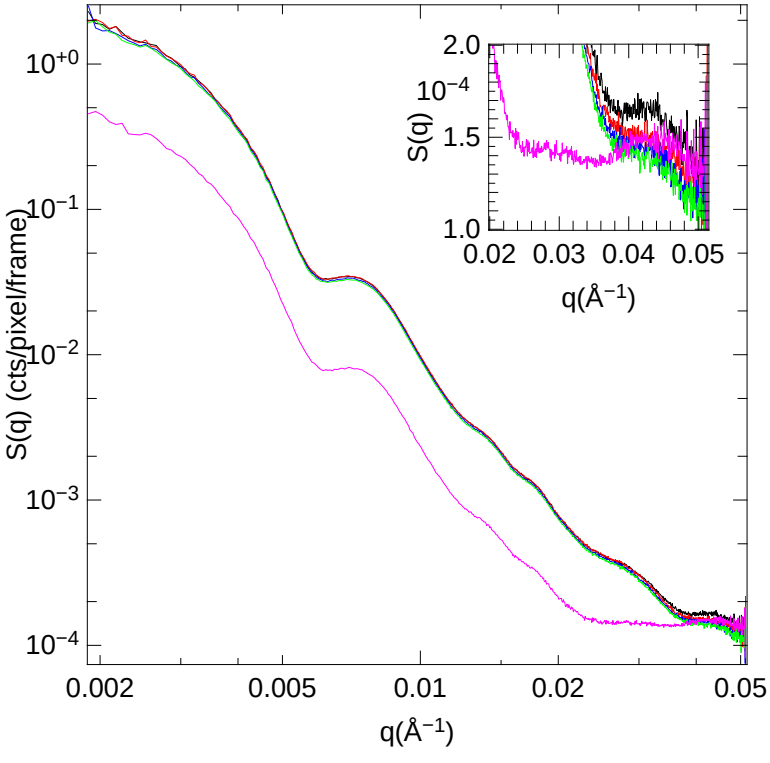
1030×1065*2*10000 is 21939 Mbytes

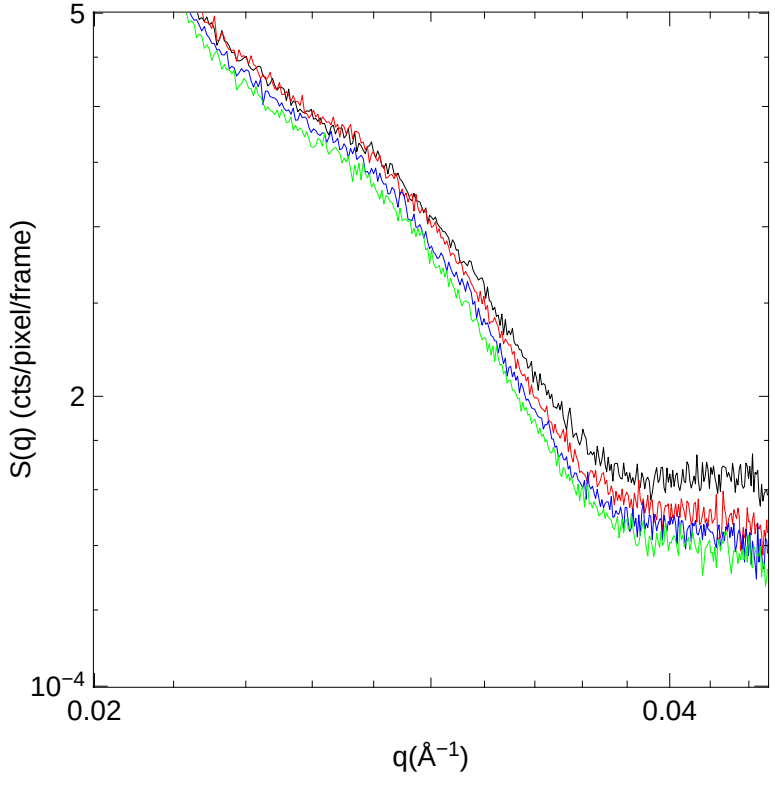
Zinger



4000 images at 1.25 msec (5 seconds of data.)

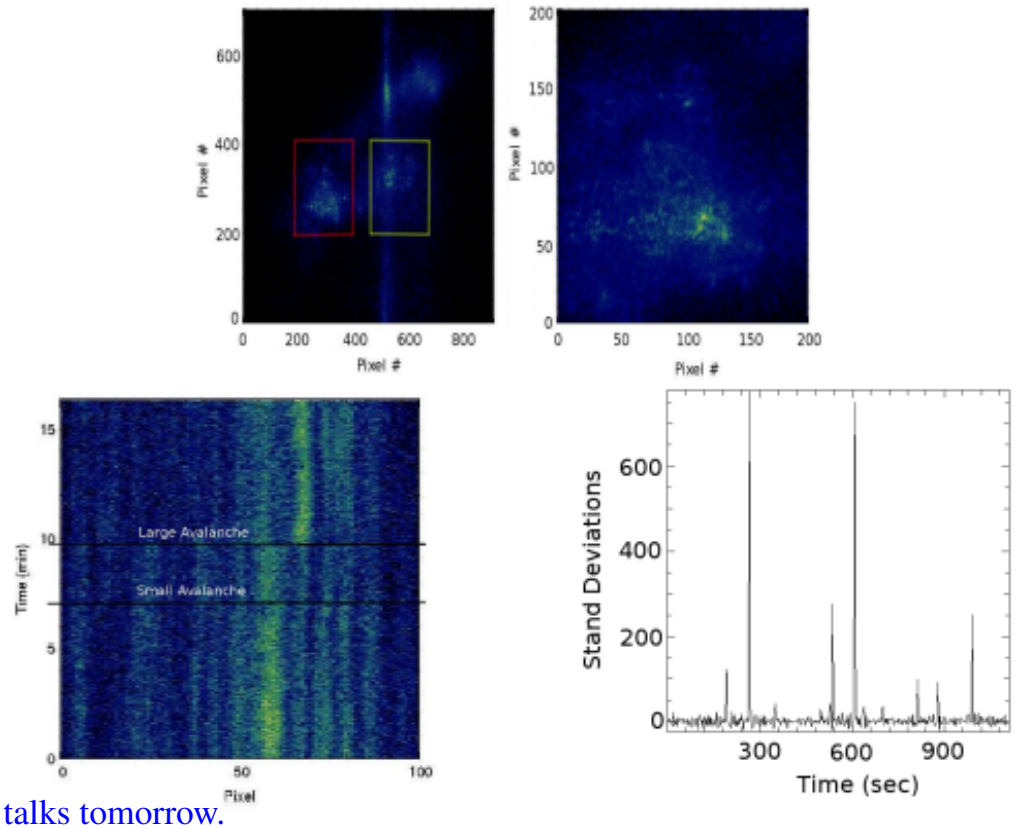
Threshold





Thresholds: 3.5 red, 3.7 black, 3.9 blue, 4.1 green, 5.0 magenta

Co: FCC to HCP transition



M. Rogers talks tomorrow.

A trigger mechanism would be nice.

Conclusion

- Eiger works great for XPCS. Measurements were done a sample–detector distance 4 m and 20x20 micron beam. At sector 8 it could be placed at 7 m and this would triple the contrast. Focussing down to 10x10 would result in $\beta = .53$
- Potential to get down to 2 microsecond resolution with visibility measurements.
- Comparing 100 Hz data too 10 Hz data shows they are equivalent for delays longer than 10. Thus there no (or little) loss by running the detector flat out.
- Control program for detector needs to be subservient to the beamline controls. Should be triggered/synchronized to scanning the spectrometer or controlled by same electronics as controls external parameters for environment (electric or magnetic fields etc). Flexibility required.